Materials Science & Engineering A 653 (2016) 147–152

Contents lists available at ScienceDirect

Materials Science & Engineering A

journal homepage: www.elsevier.com/locate/msea

Deformation-induced martensitic transformation in a 201 austenitic steel: The synergy of stacking fault energy and chemical driving force

M. Moallemi [a,*], A. Kermanpur [a], A. Najafizadeh [a,b], A. Rezaee [a], H. Samaei Baghbadorani [a], P. Dastranjy Nezhadfar [a]

[a] Department of Materials Engineering, Isfahan University of Technology, Isfahan 84156-83111, Iran
[b] Fould Institute of Technology, Fouladshahr, Isfahan, 8491663763, Iran

ARTICLE INFO

Article history:
Received 9 October 2015
Received in revised form
1 December 2015
Accepted 7 December 2015
Available online 9 December 2015

Keywords:
Stainless steels
Deformation-induced martensitic transformation
X-ray diffraction
Magnetic induction

ABSTRACT

The present study deals with the correlation of stacking fault energy's synergy and driving force in the formation of deformation-induced martensitic transformation in a 201 austenitic stainless steel. The fraction of deformation-induced martensite was characterized by means of X-ray diffraction and magnetic induction techniques. The kinetics of the martensite formation versus applied strain was evaluated through the sigmoidal model. It was shown that the volume fraction of ά-martensite is closely related to the driving force/SFE ratio of the alloy. The results also showed that the martensite content is similar in both XRD and magnetic methods and the applied sigmoidal model was consistent with the obtained experimental data.

1. Introduction

Austenitic stainless steels are traditionally used in a range of applications specifically where good corrosion resistance is required. In metastable austenitic stainless steels, γ-austenite (fcc, paramagnetic) can transform to the martensite during deformation. In fact, the austenite phase in these grades is normally not a stable phase. [1–13]. Two types of martensite can form during the deformation of metastable alloys; hexagonal close-packed ε-martensite and body-centered tetragonal ά-martensite. It has been reported that the most likely mechanism for the martensitic transformation in metastable austenitic steels is $\gamma \rightarrow \varepsilon \rightarrow \acute{\alpha}$ [10,13]. Indeed, During the early stages of deformation, shear bands including stacking faults and ε-martensite form on the {111} planes of austenite [10,13,14]. By increasing deformation, α′-martensite grows at the expense of consuming the ε-martensite and austenite phases [6,10]. However, in some of metastable alloys, the α′-martensite can directly form from the austenite phase. Das et al. [15] perceived that the nucleation of martensite in 304 LN stainless steel can successfully occur also at locations other than intersecting shear bands, and multiple mechanisms such as $\gamma \rightarrow \varepsilon$, $\gamma \rightarrow \acute{\alpha}$, and $\gamma \rightarrow \varepsilon \rightarrow \acute{\alpha}$ can happen in the microstructure simultaneously. Therefore, the nucleation of ά-martensite can be independent of ε-martensite during deformation in some conditions. The transformation of γ-austenite to ά-martensite increases the strain hardening rate and leads to a higher ultimate tensile strength. In addition, the small amount of α′-martensite decreases the work-hardening rate and ultimate tensile strength. Moreover, the elongation is affected by the rate of α′-martensite transformation [16]. Hence, the characterization of martensitic transformation behavior is an essential constituent to control forming processes efficiently.

It is well reported in the literature that the stacking fault energy (SFE) has a main role in controlling deformation mechanisms in metastable austenitic steels. In fact, the strain-induced phenomena such as twinning-induced plasticity (TWIP), and/or transformation-induced plasticity (TRIP) are strongly dependent on the SFE value [17]. Generally, in the low SFE alloys the martensitic transformation (ε or ά-martensite) i.e. the TRIP phenomenon, is the predominant plasticity mechanism. In fact, there is a boundary value for the SFE in metastable austenitic steels as the upper limit to the formation of martensite. Sato et al. [18] found that in Fe–Mn–Al alloys, high stacking fault energy (SFE) (more than 20 mJ/m^2) promotes the direct transformation $\gamma \rightarrow \acute{\alpha}$, while a low SFE (lower than 20 mJ/m^2) leads to the transformation $\gamma \rightarrow \varepsilon \rightarrow \acute{\alpha}$. It should be noted that different values have been reported for the upper limit of SFE for the martensite transformation during deformation. These discrepancies are related to the differences in the chemical composition of the studied alloys, density and configuration of dislocations, grain size and the method of SFE

* Corresponding author.
E-mail address: m.moallemi@ma.iut.ac.ir (M. Moallemi).

http://dx.doi.org/10.1016/j.msea.2015.12.006
0921-5093/

measurement [10,19–21].

As mentioned before, in most of the investigations, SFE is considered as the most important parameter for the formation of martensite during deformation. Although the lower SFE favors the formation of deformation-induced martensite (DIM), it seems that it is not a sufficient condition for the nucleation ά-martensite. The recent studies [8,10] have revealed that, in addition to SFE, the driving force for the γ→ά transformation is another effective parameter on the formation of deformation induced martensite (DIM). However, based on the author's knowledge of the literature, an extensive investigation about the correlation of the synergy between SFE and the γ→ά transformation driving force in the formation of deformation-induced martensite in austenitic stainless steels, has not been conducted so far. Consequently, the aim of this paper is to investigate the correlation between SFE and the driving force in the formation of deformation-induced martensite in a metastable 201 stainless steel. For this aim, the volume fraction of martensite with applied strain was measured by XRD and magnetic induction methods and the austenite stability was explored in comparison with a series of commercial stainless steels. The kinetics of the martensite formation is also investigated.

2. Materials and experimental procedures

The 201 austenitic stainless steel slabs with chemical composition (in wt%) of Fe–0.08C–0.54 Si–5.91 Mn–16.6 Cr–3.73 Ni–0.04N were prepared using an induction furnace under air atmosphere. The cast ingots were hot forged at the temperature range of 1000–1200 °C after a homogenization treatment at 1200 °C for 15 h. Several specimens with the dimensions of $50 \times 20 \times 8$ mm^3 were then machined for the subsequent solution annealing and cold rolling processes. The multi-pass unidirectional cold rolling was carried out in a two-high rolling mill under oil lubrication. Different thickness reductions from 5% to 90% were carried out at room temperature (25 °C).

The phase characterization was conducted during cold rolling by a Ferritescope (Fischer MP30) and X-ray diffractometer (XRD, Philips X'Pert with Cu K_α mode). The microstructures were observed using optical microscopy. The cold-rolled specimens were etched in a mixture containing two solutions in 1:1 ratio: 0.20% sodium-metabisulfate and 10% hydrochloric acid to reveal the α′-martensite phase.

The quantitative estimation of phases by XRD was conducted by direct comparison method. In this method, the total integrated intensity of all diffraction peaks for each phase in a mixture is proportional to the volume fraction of that phase. If grains of each phase are randomly oriented, the integrated intensity '*I*' of any diffraction peak from phase 'i' will be given by [22]:

$$I_i^{hkl} = \frac{KR_i^{hkl}V_i}{2\mu} \tag{1}$$

where;

$$R_{hkl} = \left(\frac{1}{v^2}\right)\left[|F|^2 p\left(\frac{1+\cos^2\theta}{\sin^2\theta\cos\theta}\right)\right]\left(e^{-2M}\right) \tag{2}$$

$$K = \left(\frac{I_0 A\lambda^3}{32\pi r}\right)\left[\left(\frac{\mu_0}{4\pi}\right)\frac{e^4}{m^2}\right] \tag{3}$$

I_i^{hkl}: integrated intensity for the (*hkl*) plane of *i*-phase, *i*: γ or α′, *K*: the instrument factor, R_i^{hkl}: material scattering factor that depends on θ, interplanar spacing of *hkl*, composition and the crystal structure of the phase *i*, V_i: volume fraction of phase *i*, ν: volume of unit cell, F_{hkl}: structure factor for the reflecting plane (*hkl*), *p*: multiplicity factor, e^{-2M}: temperature factor, *k*: the wavelength of incident X-ray beam, μ: linear absorption coefficient, *A*: cross sectional area of the incident X-ray beam, I_0: intensity of the incident beam, *r:* radius of the diffractometer circle, *e* and *m*: charge and mass of electron, respectively.

Therefore, for a steel containing γ-austenite and α′-martensite, Eq. (1) can be written as:

$$I_\gamma = \frac{KR_\gamma V_\gamma}{2\mu},\ I_{\alpha'} = \frac{KR_{\alpha'}V_{\alpha'}}{2\mu},\ I_\varepsilon = \frac{KR_\varepsilon V_\varepsilon}{2\mu} \tag{4}$$

considering the following relationship

$$V_\gamma + V_\varepsilon + V_{\alpha'} = 1 \tag{5}$$

and knowing that $K/2\mu$ is constant in a given X-ray diffraction scan, the volume fraction of the individual phases can be calculated by:

$$V_i = \frac{\frac{1}{n}\sum_{j=1}^{n}\frac{I_i^j}{R_i^j}}{\frac{1}{n}\left(\sum_{j=1}^{n}\frac{I_\gamma^j}{R_\gamma^j} + \sum_{j=1}^{n}\frac{I_{\alpha'}^j}{R_{\alpha'}^j} + \sum_{j=1}^{n}\frac{I_\varepsilon^j}{R_\varepsilon^j}\right)} \tag{6}$$

where i=γ, ά or ε and *n* is the number of peaks examined.

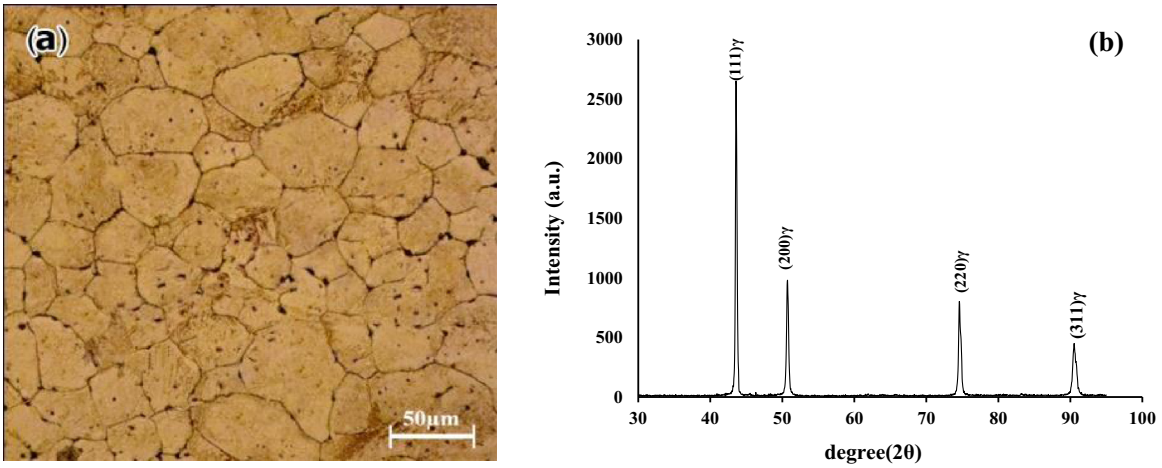

Fig. 1. (a) Optical micrograph and (b) XRD pattern of a solution annealed specimen.